

Temperature-Induced Semiconducting $c(4 \times 2) \Leftrightarrow$ Metallic (2×1) Reversible Phase Transition on the β -SiC(100) Surface

V. Yu. Aristov,* L. Douillard, O. Fauchoux, and P. Soukiassian

Commissariat à l'Energie Atomique, DSM-DRECAM-SRSIM, Bâtiment 462, Centre d'Etudes de Saclay, 91191 Gif sur Yvette Cedex, France

and Département de Physique, Université de Paris-Sud, 91405 Orsay Cedex, France

(Received 27 May 1997)

We use combined variable temperature scanning tunneling microscopy and spectroscopy, and angle-resolved photoemission spectroscopy experiments to study transition between two β -SiC(100) surface structures. We observe a reversible temperature-dependent phase transition from a semiconducting $c(4 \times 2)$ surface at 25 °C to a metallic 2×1 structure at 400 °C. This transition results from temperature-induced disruption of the $c(4 \times 2)$ structure composed of alternately up and down dimers into a structure having all dimers at the same height giving a 2×1 symmetry. This arrangement favors electronic orbital overlap between Si top surface atoms leading to surface metallization. [S0031-9007(97)04495-5]

PACS numbers: 68.35.Rh, 61.16.Ch, 79.60.Bm

Surface reconstructions and phase transitions are widely investigated topics by various experimental techniques and/or theoretical approaches. In fact, their understanding is very important from a fundamental aspect but is also very useful to achieve specific surface properties. In contrast to metals, there are very few reversible surface phase transitions for semiconductors limited to silicon and germanium only [1–5]. The low to room temperature reversible transition from $c(4 \times 2)$ to 2×1 reconstructions for Si(100) and Ge(100) surfaces is of particular interest and has been intensively investigated as a model case [1–5]. This phase transition was shown to result from switching between anticorrelated to correlated asymmetric dimers [2–5]. Also, reversible order-disorder phase transitions such as 7×7 (8×2) to 1×1 for Si (Ge) (111) surfaces and 2×1 to 1×1 for Si and Ge (100) surfaces occur at elevated temperatures [3]. Recently, the Si(100)-(2×1) surface was found to exhibit a metallic-like character above a surface temperature of 625 °C with the surface keeping the same 2×1 symmetry [6]. This metallic transition was shown to result from Si-dimer flipping dynamics [6]. Understanding the mechanisms leading to surface metallization is indeed a very important fundamental issue, as well as being driven by its technological importance, especially for semiconductor surfaces.

Silicon carbide (SiC) is a very interesting wide band-gap IV-IV compound semiconductor having many advanced applications in sensors and electronics, especially for high temperature, high power, high speed, and high voltage devices [7]. It is only recently that significant progress has been made into the knowledge of its surfaces. Lately, room temperature scanning tunneling microscopy (RT-STM), synchrotron radiation photoemission experiments, and *ab initio* theoretical calculations have brought very novel insights about cubic (β) SiC(100) surface atomic geometry [7–12]. Contrary to Si(100) and Ge(100) which have stable 2×1 reconstructions at 25 °C [1–4], the β -

SiC(100) surface exhibits instead a $c(4 \times 2)$ reconstruction [8,9]. The latter has a very different atomic geometry from the low temperature Si(100) and Ge(100) $c(4 \times 2)$ reconstructions [2–5]. The β -SiC(100) $c(4 \times 2)$ surface results from dimer rows having alternately up and down dimers (AUDD model) within the row [8]. This very particular atomic arrangement reduces the large surface stress for Si surface atoms which, due to very different lattice parameters when compared to Si(100), are compressed by $\approx 20\%$ [8]. Contrary to previous knowledge, the β -SiC(100)-(2×1) reconstruction seems to result from slight contamination or high defect densities of $c(4 \times 2)$ surfaces [7–9]. Unlike elemental semiconductors, no reversible surface phase transition has ever been observed so far for compound semiconductors.

In this Letter, we use variable temperature scanning tunneling microscopy and spectroscopy (VT-STM and VT-STs), and angle-resolved ultraviolet photoemission spectroscopy (VT-ARUPS) to show evidence of the first reversible surface phase transition for a compound semiconductor. This temperature-induced transition occurs for β -SiC(100) from a semiconducting $c(4 \times 2)$ reconstruction at 25 °C to a metallic 2×1 one at 400 °C. It is found to result from the AUDD arrangement disruption leading to a 2×1 surface with metallization originating from surface atom electronic orbital overlap.

The experiments are performed using two different systems, one with an Omicron VT-STM operating from -230 to $+900$ °C, and the other with an angle resolved CLAM 2 (VG) hemispherical electron analyzer and an ultraviolet plasma source for photoemission experiments. The pressure in the STM chamber is always $\leq 4 \times 10^{-11}$ torr at room temperature and 9×10^{-11} torr at a 400 °C sample temperature. In the photoemission chamber, the base pressure is always $\leq 8 \times 10^{-11}$ torr. The surface structure is double-checked by low energy electron diffraction (LEED) attached to both systems. A tungsten tip is used (sample

grounded) for STM and STS while an ≈ 60 min stabilization time is necessary for temperature-dependent measurements. All STM topographs are obtained by tunneling from the filled electronic states of the sample. We were not able to obtain atom-resolved empty-electronic state STM topographs. Other experimental details about high quality β -SiC(100) surface preparation, in particular for the $c(4 \times 2)$ reconstruction, are available elsewhere [8].

We first look at a representative room temperature (RT) $100 \text{ \AA} \times 100 \text{ \AA}$ STM topograph (filled states) of the $c(4 \times 2)$ surface [Fig. 1(a)] exhibiting the characteristic β -SiC(100) $c(4 \times 2)$ surface pseudohexagonal pattern with each spot representing a Si dimer as shown in our previous RT-STM study [8]. The corresponding LEED photograph is also shown at the bottom right-hand corner of Fig. 1(a).

Next, we investigate the effect of temperature on surface ordering by maintaining the sample at high temperatures. Figure 1(b) displays a $100 \text{ \AA} \times 100 \text{ \AA}$ STM topograph for a surface temperature of $400 \text{ }^\circ\text{C}$ with the corresponding LEED photograph displayed as an inset at the bottom right-hand corner. At this temperature, the LEED pattern clearly arises from a 2×1 surface reconstruction. The STM topograph shows that the corrugation somewhat deteriorates along dimer rows, suggesting an arrangement characteristic of a 2×1 ordering (as observed for defect-induced 2×1 domains [8]), in agreement with the LEED pattern. The observation of a 2×1 LEED pattern at $400 \text{ }^\circ\text{C}$ indicates a long range surface ordering. When following the LEED pattern starting from a 2×1 array (at $400 \text{ }^\circ\text{C}$) and letting the surface cool, one can observe the appearance of additional diffuse large spots giving rise to the full $c(4 \times 2)$ LEED pattern when the surface is back at RT. Similarly, the STM topograph correlates with LEED observation and shows a $c(4 \times 2)$ surface reconstruction when the surface is cooled to RT. These features indicate the reversible nature of this phase transition.

To get deeper insights about this interesting $c(4 \times 2) \leftrightarrow 2 \times 1$ reversible phase transition, we explore the electronic properties by scanning tunneling spectroscopy (STS), which is a very powerful tool to probe surface insulating vs metallic behavior [2]. We perform I - V measurements at RT and at $400 \text{ }^\circ\text{C}$, at tip to sample bias in the -4 to $+4$ V range. Figure 2 exhibits such I - V characteristics for the $c(4 \times 2)$ ($25 \text{ }^\circ\text{C}$) and 2×1 ($400 \text{ }^\circ\text{C}$) surface reconstructions. Such curves represent an average of I - V curves measured at 3 \AA grid spacings over the $100 \text{ \AA} \times 100 \text{ \AA}$ surface. The $c(4 \times 2)$ I - V curve (a) recorded at $25 \text{ }^\circ\text{C}$ exhibits an ≈ 1.7 V horizontal flat section (the bulk β -SiC gap is 2.3 eV [7]), clearly indicating the surface semiconducting nature. In strong contrast, the 2×1 I - V curve (b) recorded at $400 \text{ }^\circ\text{C}$ is almost linear and does not show any measurable gap. This very interesting feature indicates that the temperature-induced 2×1 surface reconstruction has a metallic character, thereby explaining the observed decrease in corrugation for the 2×1 STM topograph [Fig. 1(b)].

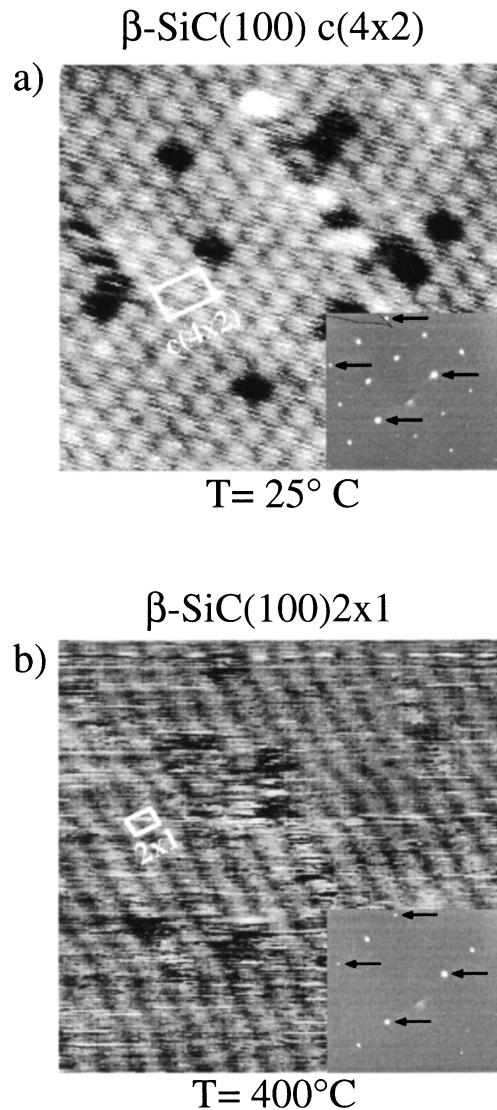


FIG. 1. $100 \text{ \AA} \times 100 \text{ \AA}$ STM topographs (filled states): (a) β -SiC(100) $c(4 \times 2)$ at $25 \text{ }^\circ\text{C}$ and (b) β -SiC(100)-(2×1) at $400 \text{ }^\circ\text{C}$. The tip bias was $+3.2$ eV at a 0.12 nA tunneling current. The corresponding LEED photographs ($E_p = 60$ eV) are also displayed as insets at the bottom right-hand corner of (a) and (b) with arrows indicating the 1×1 spots.

Additional information about this striking temperature-induced $c(4 \times 2) \leftrightarrow 2 \times 1$ phase transition could be found by looking at the electronic properties. However, the electronic structure of the β -SiC(100) $c(4 \times 2)$ surface reconstruction has basically never been investigated either experimentally or theoretically. We have therefore comprehensively studied the electronic structure of this $c(4 \times 2)$ surface reconstruction by ARUPS [13]. Of particular interest to the scope of the present work is an electronic surface state specific of the $c(4 \times 2)$ reconstruction [13]. Figure 3 displays a representative valence band spectrum recorded at 12° off-normal emission along the $\langle 110 \rangle$ direction showing an electronic state located at 1.3 eV below the Fermi level. This electronic state is destroyed at a low oxygen exposure (Fig. 3) and exhibits

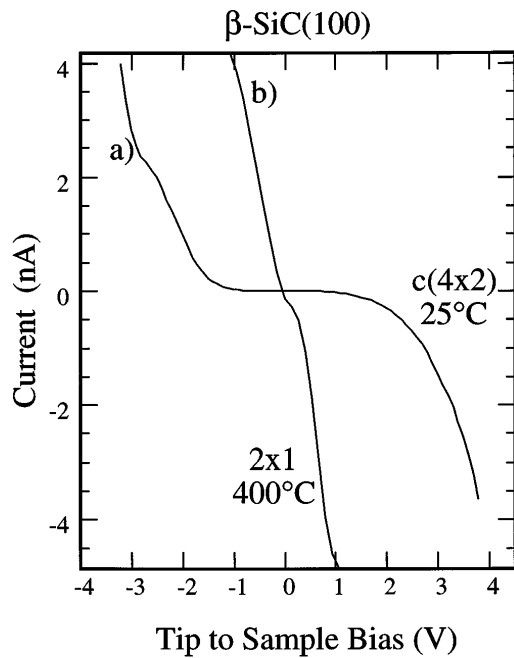


FIG. 2. Tunneling current vs voltage STS (I - V) for (a) β -SiC(100) $c(4 \times 2)$ at 25 °C and (b) β -SiC(100)- (2×1) at 400 °C. Each curve represents an average of 1000 I - V characteristics recorded on a grid by equal steps all over the $100 \text{ \AA} \times 100 \text{ \AA}$ surface. Both curves were recorded using the same tip to sample distance. The sample is grounded.

the same energy dispersion vs k_{\parallel} for different photon energies (He I at 21.2 eV and Ne I at 16.85 eV) [13] which indicate that this 1.3 eV spectral feature is a surface state. Since this surface state is characteristic of the $c(4 \times 2)$ reconstruction [13], one can expect it to be dramatically affected by any structural change, such as phase transition. We now study the behavior of this surface state from 400 to 25 °C to get additional information about this temperature-induced $c(4 \times 2) \Leftrightarrow 2 \times 1$ transition. Photoemission spectra in Fig. 4 are recorded in a region centered around 1.3 eV binding energy. We start from the 2×1 reconstruction at a surface temperature of 400 °C, and let the surface cool to 25 °C until a $c(4 \times 2)$ surface reconstruction is again observed. While no similar surface state is seen at 400 °C for the metallic 2×1 surface, it is developing (already from spectrum #2 in Fig. 4, i.e., just after initial temperature decrease) when cooling until 25 °C, showing the same shape specific of the semiconducting $c(4 \times 2)$ surface. This behavior correlates with the $c(4 \times 2) \Leftrightarrow 2 \times 1$ reversible phase transition. The gradual increase of the $c(4 \times 2)$ surface state intensity with decreasing temperatures suggests that the $2 \times 1 \Leftrightarrow c(4 \times 2)$ transition is not sharp, likely implying the existence of mixed $c(4 \times 2)$ and 2×1 domains.

Our results above support a picture of temperature-induced semiconducting $c(4 \times 2) \Leftrightarrow$ metallic 2×1 phase transition for the β -SiC(100) surface. Starting from the RT $c(4 \times 2)$ AUDD structure, increasing temperatures induce vibrational effects leading to the 2×1 surface arrangement observed by VT-STM and LEED at 400 °C

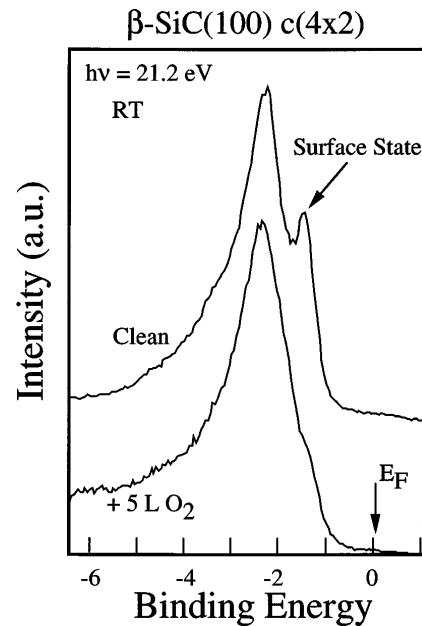


FIG. 3. Representative ARUP spectrum at 12° off normal emission along the $\langle 110 \rangle$ direction recorded for β -SiC(100) $c(4 \times 2)$ surfaces: (i) clean (top) and (ii) after a 5 L O_2 (1 L = 1 langmuir = 10^{-6} Torr sec) exposure (bottom). The photon energy is 21.2 eV. The specific $c(4 \times 2)$ surface state located at a 1.3 eV binding energy, which shows the same energy dispersion vs k_{\parallel} for different photon energies (16.85 and 21.2 eV) [13], is destroyed by low O_2 exposures.

[Fig. 1(b)] in which all dimers are on average at the same height (Fig. 5). In this configuration, the distance between Si dimers belonging to the same row would be decreased to its minimum value at 3.08 Å. This would in turn significantly increase the overlap between surface atom electronic orbitals favoring a metallic character of this surface as observed by STS. Such a mechanism would induce a significant electronic redistribution within the top Si layer, thus explaining quenching of the $c(4 \times 2)$ surface state (Fig. 4).

The behavior of the Si(100)- (2×1) surface at high temperatures is also of special interest in the present context [6]. In this case, a surface temperature of ≈ 625 °C results in asymmetric dimer flipping around a symmetric dimer position (with the same 2×1 LEED pattern) leading to dynamically induced surface metallization [6]. A similar mechanism involving dynamically induced metallization cannot be ruled out here for the β -SiC(100)- (2×1) surface at 400 °C, probably with different vibration modes. However, it is interesting to remark that the present temperature-induced β -SiC(100) surface metallization results from a structural $c(4 \times 2)$ to 2×1 reversible phase transition, unlike the Si(100)- (2×1) surface which maintains the same 2×1 symmetry for both semiconducting and metallic states [6].

Cooling the β -SiC(100)- (2×1) surface down to RT leads to the original AUDD arrangement for Si dimers associated with the semiconducting $c(4 \times 2)$ reconstruction. The corresponding appearance of the $c(4 \times 2)$

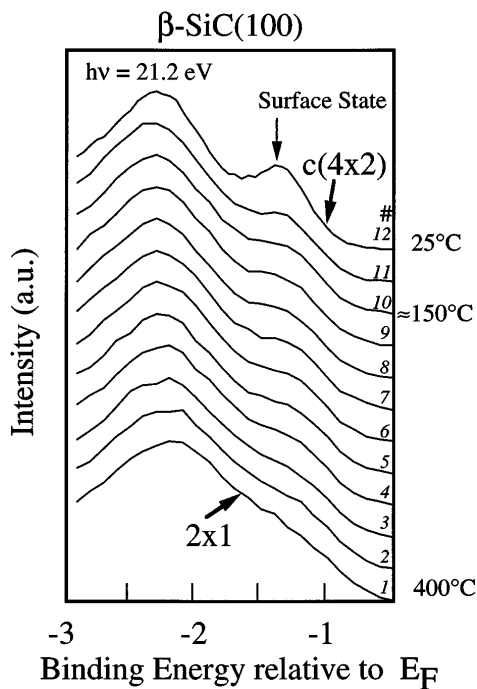


FIG. 4. ARUP spectra for Si-terminated β -SiC(100) recorded at various surface temperatures in the region centered around the $c(4 \times 2)$ surface state shown in Fig. 3. The spectra are recorded during sample cooling from 400°C (2×1 reconstruction) and to 25°C [$c(4 \times 2)$ reconstruction]. Time intervals between spectra are, respectively, 8 sec between curves #1–#10, 80 sec between curves #10 and #11, and 45 min between curves #11 and #12. The photon energy is 21.2 eV.

related electronic surface state (Fig. 4) further demonstrates that this behavior is correlated to the phase transition. One should also notice that the 2×1 surface reconstruction is achieved at the rather low surface temperature of 400°C. Interestingly, our recent *ab initio* calculations show that the β -SiC(100) $c(4 \times 2)$ and the 2×1 structures have a very small energy difference (a few kT), despite significant differences in atomic heights [14]. This indicates the rather low energy necessary to initiate this transition leading to the 2×1 metallic surface reconstruction observed at 400°C.

In conclusion, we provide evidence of the first reversible surface phase transition for a compound semiconductor. A temperature-induced semiconducting $c(4 \times 2) \Leftrightarrow$ metallic 2×1 reversible phase transition is observed for the β -SiC(100) surface by variable temperature scanning tunneling microscopy and spectroscopy, and by angle-resolved ultraviolet photoemission experiments. This transition results from the disruption of the $c(4 \times 2)$ surface reconstruction in the AUDD arrangement leading to all dimers having the same height. Subsequent electronic orbital overlap between surface Si atoms, in which surface vibrations also play a role, is at the origin of surface metallization.

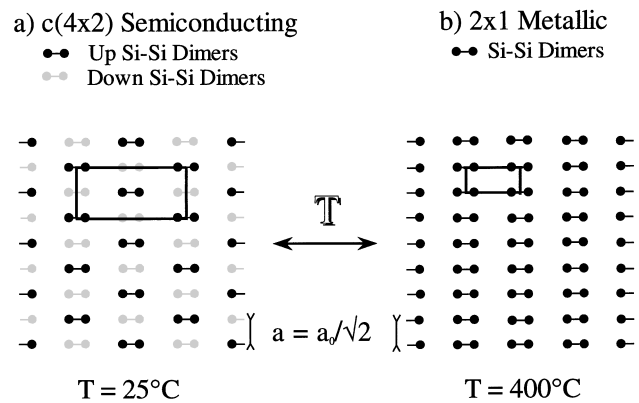


FIG. 5. Schematic of the reversible β -SiC(100) surface phase transition from a semiconducting $c(4 \times 2)$ reconstruction having dimer rows of up and down dimers (AUDD) to a 2×1 metallic one having all dimers at the same height. The corresponding surface unit cells are also indicated.

The authors are grateful to E. Wimmer for very fruitful discussions and to L. di Cioccio, C. Jaussaud, and C. Pudda at LETI (CEA-Technologies Avancées, Grenoble) for providing β -SiC(100) samples.

*On leave from Institute of Solid State Physics, Russian Academy of Sciences, Chernogolovka, Moscow district, Russia, 142432.

- [1] C. B. Duke, Chem. Rev. **96**, 1237 (1996), and references therein.
- [2] J. A. Kubby and J. J. Boland, Surf. Sci. Rep. **26**, 63 (1996), and references therein.
- [3] W. Mönch, *Semiconductor Surfaces and Interfaces* (Springer-Verlag, Berlin, Heidelberg, 1993), and references therein.
- [4] J. P. LaFemina, Surf. Sci. Rep. **16**, 133 (1992), and references therein.
- [5] R. A. Wolkow, Phys. Rev. Lett. **68**, 2636 (1992).
- [6] L. Gavioli, M. G. Betti, and C. Mariani, Phys. Rev. Lett. **77**, 3869 (1996).
- [7] R. Kaplan and V. M. Bermudez, in *Properties of Silicon Carbide*, edited by G. Harris, EMIS Datareview Series (INSPEC, London, 1995), Vol. 13, p. 101, and references therein.
- [8] P. Soukiassian, F. Semond, L. Douillard, A. Mayne, G. Dujardin, L. Pizzagalli, and C. Joachim, Phys. Rev. Lett. **78**, 907 (1997).
- [9] M. L. Shek, Surf. Sci. **349**, 317 (1996).
- [10] P. Käckell, J. Furthmüller, and F. Bechstedt, Appl. Surf. Sci. **104–105**, 45 (1996).
- [11] M. Sabisch, P. Krüger, A. Mazur, M. Rohlfiing, and J. Pollmann, Phys. Rev. B **53**, 13 121 (1996).
- [12] A. Catellani, G. Galli, and F. Gygi, Phys. Rev. Lett. **77**, 5090 (1996).
- [13] V. Yu. Aristov and P. Soukiassian, recent angle-resolved photoemission experiments.
- [14] L. Douillard, B. Delley, P. Soukiassian, and E. Wimmer, recent *ab initio* DMol calculations.